

# AUTOMATION OF PAVEMENT SURFACE CRACK DETECTION WITH A MATCHED FILTERING TO DEFINE THE MOTHER WAVELET FUNCTION USED

Peggy Subirats (1), Jean Dumoulin(1), Vincent Legeay(1) and Dominique Barba(2)

(1)Laboratoire Central des Ponts et Chaussées, Route de Bouaye BP 4129 44341 Bouguenais Cedex (France),  
Email: {peggy.subirats,jean.dumoulin,vincent.legeay}@lcpc.fr

(2)Institut de Recherche en Communications et Cybernétique de Nantes, École polytechnique de l'Université de Nantes rue  
Christian Pauc La Chantrerie BP 60601 44306 Nantes Cedex (France),  
Email:dominique.barba@polytech.univ-nantes.fr

## ABSTRACT

*This paper presents a new approach in automation for crack detection on pavement surface images. The method is based on the continuous wavelet transform. In the first step, a 2D continuous wavelet transform for several scales is performed. Complex coefficient maps are built. The angle and modulus information are used to keep significant coefficients. The mother wavelet function is defined using a matched filtering, thus the method is self-adapted to the road texture. No user intervention is needed. Then, wavelet coefficients maximal values are searched and their propagation through scales is analyzed. Finally, a post-processing gives a binary image which indicates the presence or not of cracks on the pavement surface image.*

## 1. INTRODUCTION

The French road network ages. Furthermore, road traffic increase and costs of road maintenance rise. So it's important to detect defaults before the repair costs are too high. Pavement distresses are essentially due to heavy vehicle traffic and weather conditions. Nowadays, in France, thousand kilometers of roads are investigated each year. Currently, distress survey is made essentially by visual inspection. For this, qualified technicians drive in a vehicle whose speed is about 5 or 10 kilometers per hour and use an on board dedicated acquisition device. It goes without saying that this method is far to be safe, not only for road monitoring staff but also for road users. Due to the unceasing traffic increase, the automation of pavement surface distress monitoring is more and more required. One of the most promising techniques is to use image processing applied to pavement surface images previously acquired on road by a dedicated monitoring vehicle [1].

Most of image processing approaches depend on texture. They are frequently based on thresholding or filtering and frequently it's need to adapt the threshold or the filter support to the texture ([2] and [3]). Such approaches reduce the crack detection performances (thin cracks are not detected) when pavement surface texture raised up.

To our knowledge few publications are available in literature for emergent crack detection by using wavelet-based image processing method ([4], [5] and [6]). In this paper, after the problem position and a brief presentation of pavement sur-

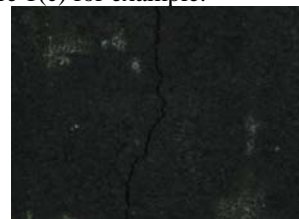
face images, we expose a new approach for automation of crack detection using a 2D wavelet-based image processing method. Some results are shown and analyzed. Finally, conclusion and perspectives are given.

## 2. PROBLEM POSITION

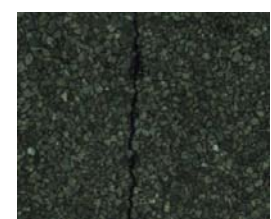
Pavement crack detection is a difficult edge detection problem due to various pavement textures that can be encountered on pavement surface images. A way to reduce the texture effect is to use low spatial resolution images. But low resolution tends to erase thin crack signatures. So, they won't be detected by image segmentation. Consequently, we have chosen to work with images whose spatial resolution is between 1 and 2 mm per pixel. If we look forward to the final on road operational system, such spatial resolution seems to be realistic, due to available technologies on the market.

Examples of pavement surface images are given on figure 1. Images (a) and (b) are laboratory images. A bituminous concrete, whose aggregate maximum size is 14 mm, is given in image (a). A pavement wearing course with surface dressing whose aggregate size are 6/10 mm and 2/4 mm is displayed in image (b). Figure 1 (c) represents an image of a circulated road acquired in static mode with an alligator cracking on its surface. Figure 1 (d) represents an image of a circulated road acquired in static mode with a crack in a star shape on its surface.

Figure 1 also illustrates problems that may be encountered during the crack detection process. A major problem is the road texture. Indeed, for strong textures (like this represented figure 1 (b)), some spaces between aggregates are wider than the crack itself, so in such conditions it's hard to detect the default. A second important difficulty is lighting conditions, the cast shadows problem is represented in figure 1(c) for example.



(a)



(b)



Figure 1: example of laboratory images (a and b) and real road images (c and d)

### 3. THE WAVELET-BASED IMAGE PROCESSING METHOD FOR CRACK DETECTION

In this paragraph, we describe the proposed wavelet-based method for pavement surface crack detection. Some illustrations of results obtained at different steps of this method are given.

#### 3.1 The proposed method

A general scheme of the proposed method is given onto figure 2.

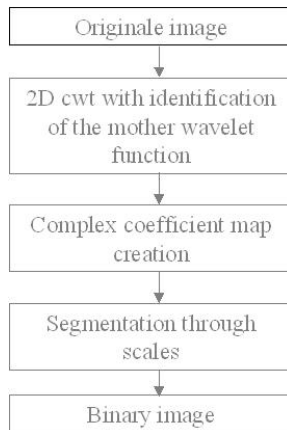


Figure 2: scheme of the image processing method proposed for pavement crack detection

This method can be divided in three steps from the original pavement image surface to be analyzed to the pavement crack map binary image generated.

The first step use the 2D continuous wavelet transform (CWT) [7] applied to pavement surface image. We only remind here the 2D CWT expression:

$$\begin{aligned}
 Wf(a, \vec{b}, \theta) &= \iint_{\mathbb{R}^2} f(\vec{x}) \psi_{(a, \vec{b}, \theta)}^*(\vec{x}) d\vec{x} \\
 &= \frac{1}{a} \iint_{\mathbb{R}^2} f(\vec{x}) \psi(R^{-\theta}(\frac{\vec{x} - \vec{b}}{a})) d\vec{x}
 \end{aligned}$$

Where :

The base atom  $\psi$  is a zero average function, centered around zero and of a finite energy,  $a$  the scale parameter and  $b$  the translation parameter.

During this first step the 2D CWT is only performed for both the  $0^\circ$  and the  $90^\circ$  directions and at several scales.

#### 3.2 Choice for the mother wavelet function

The choice for the wavelet mother function depends on the application. The problem here, as presented in paragraph 2, is the various number of road textures. So, the usual wavelet functions (mexican hat, symlet...) don't give the same results for all textures. Yet, our goal is to automate the crack detection independently of the road surface. So, no user has to intervene in the process.

So, the idea here is to define the mother wavelet function for each road image in order to adapt it to the texture. For this, we perform a matched filter and interpolated the discret filter to obtain a continuous function, which is our mother wavelet function.

The signal that interests us is defined as followed:  $\{z_i\} = \{s_i\} + \{b_i\}$  where :

- $i = 1 : N$  is the sample number.
- $\{s_i\}$  is the crack signal
- $\{b_i\}$  is the texture signal which is considered as noise.

We also define  $h = \{h_i\}$  the impulse response of the filter to define and  $\varphi_{bb} = \{\varphi_{bb_n}\}$  the autocorrelation function of  $b$ .

The matched filter is the one that maximizes the signal-to-noise ratio  $\rho$  defined by:  $\rho = \frac{|h * s|^2}{E\{h * b\}^2}$  where the numerator is the power of the filtered signal and the denominator is the noise power after filtering.

Using a vectorial representation  $z = [z_N \dots z_1]$ ,  $s = [s_N \dots s_1]$ ,  $b = [b_N \dots b_1]$ ,  $h = [h_0 \dots h_N]$  and  $\Phi_{bb(i,j)} = \varphi_{bb|i-j|}$  the noise autocorrelation matrix, we have

the matched filter impulse response  $h = \Phi_{bb}^{-1} s$ .

We present here the matched filter defined for the image presented onto figure 1c. The crack model used is represented onto figure 3.

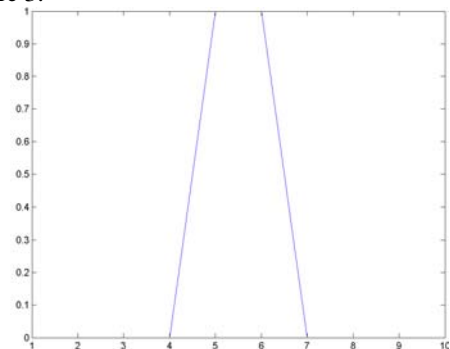


Figure 3: crack signal model

The matched filter coefficients performed for this road image are given onto figure 4. The mother wavelet function is defined by interpolated the discret signal figure 4(a) with a spline model onto 1024 points. The result is given onto figure 4(b).

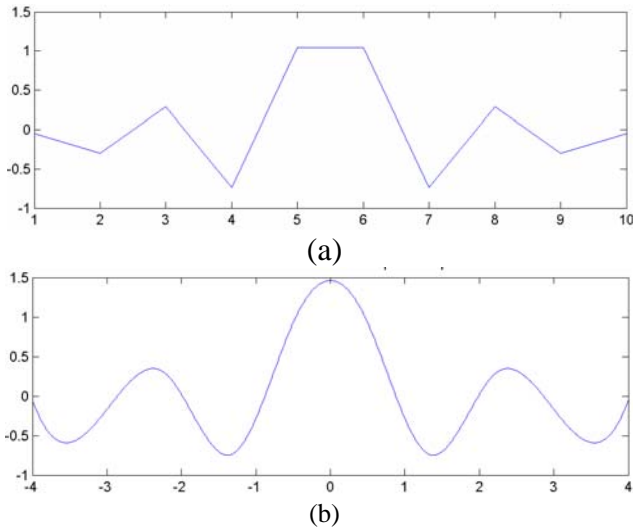


Figure 4: matched filter coefficients and the mother wavelet function

### 3.3 Complex coefficient maps creation

As we only explore two directions, a complex number was introduced in the process. The real part of this number is the result of the cwt on the direction  $90^\circ$  and the imaginary part is the result of cwt on the direction  $0^\circ$ . This step is schematized onto figure 5. From these complex coefficient maps, modulus and angles maps are built for the different scales computed.

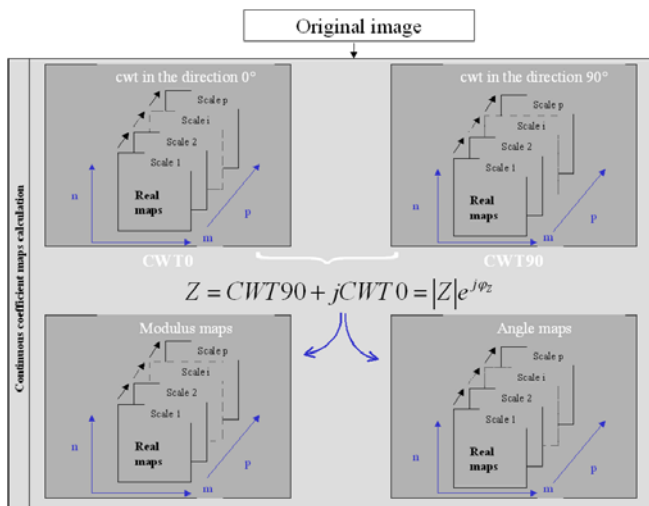


Figure 5: complex coefficient maps

As an illustration, modulus (bottom left) and phase (bottom right) maps are given onto figure 6 for the pavement image shown on the upper part.

Assuming that, on the original image, the crack is darker than the texture, such complex maps approach is useful to reduce the next segmentation step.

Due to the mother wavelet function and to the hypothesis of darker crack, coefficients corresponding to a crack must be negative for both directions. So, only modulus of coefficients whose associated angle is between  $-90^\circ$  and  $-180^\circ$  will be considered in the maxima propagation seeking. Furthermore a first threshold on low modulus value may also be applied here to eliminate low coefficient values that not match pixels belonging to a crack.

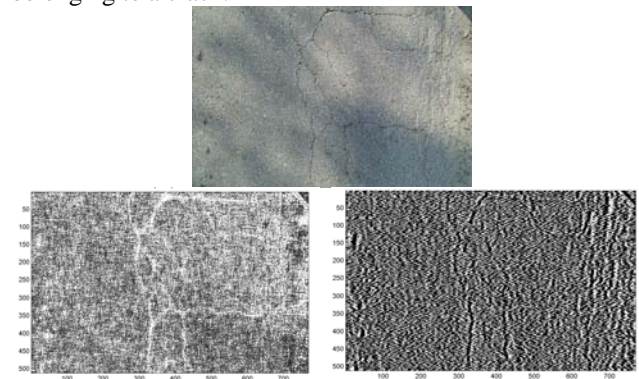


Figure 6: example of modulus and phase maps at scale 4

### 3.4 Segmentation of the wavelet coefficient maps

This segmentation step follows the maximal wavelet coefficients through scales from the largest to the smallest one.

For this, the wavelet coefficient maximal value is searched, on the modulus map at a given scale, using a 1D-structuring element whose size is the support length of the mother wavelet at this scale (9 pixels at the first scale). This search is done by sliding the structuring element with an analysis step of 1 pixel. This operation is repeated on each row and column of the modulus maps computed before. At the end, a set of maxima maps are obtained.

Figure 7 shows the location map obtain on the modulus map presented onto figure 4.

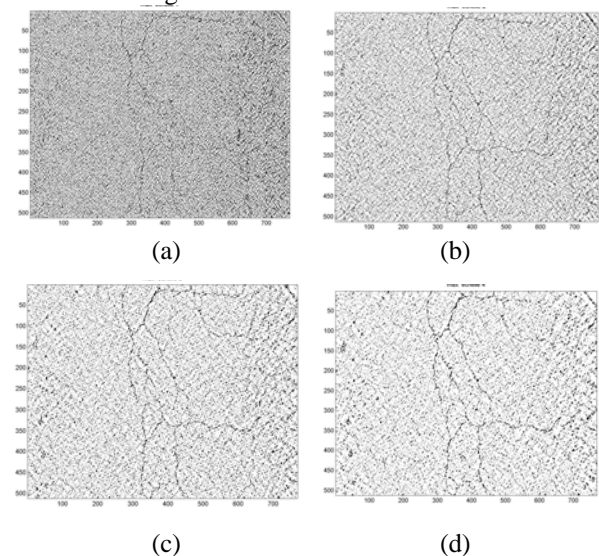


Figure 7: maxima location for scales 1 (a), 2 (b), 3 (c) and 4 (d)

As one will observed on figure 7, the map obtained is noisy due to the location procedure used that do not used at that stage the propagation information through scales.

So, in the second stage of the segmentation step, the propagation through scales is examined to go up to defaults (cracks). Figure 8 details the process of maxima research. A maximal value at scale  $p_i$  propagates if a maximal value is found in its neighborhood at scale  $p_{i-1}$ . Thus, maxima which remain at the smallest scale (scale 1 in figure 8) belong to a default.

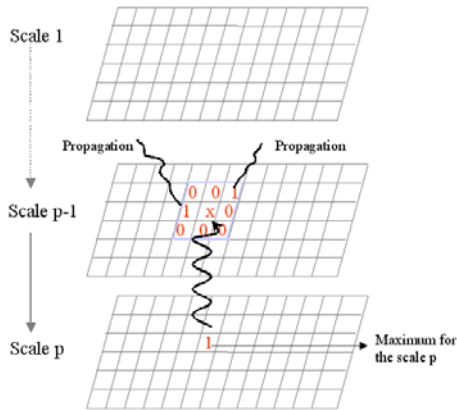


Figure 8: maxima propagation through scales

An example of result is shown onto Figure 9.

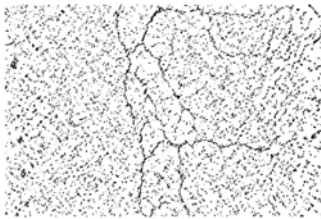


Figure 9: binary image after propagation through scales

The new map (binary image) obtained at that stage is still influenced by pavement surface texture, which induces a fragmentation of the object size detected. So post-processing is needed to reconstruct the object (crack). It consists in linking small regions to obtain larger ones before applying threshold on region size. For this, a skeletonization is performed and the end of regions is sought.

The research is done in a 5x5 structuring element around the considered end of the object and link the central pixel ( $p_{i,j}$ ) as follow:

$$\left. \begin{array}{l} p_{i-2,j-2} = 1 \\ \text{or} \\ p_{i-2,j-1} = 1 \\ \text{or} \\ p_{i-1,j-2} = 1 \end{array} \right\} \text{then, } p_{i-1,j-1} = 1 \quad \left. \begin{array}{l} p_{i-2,j+1} = 1 \\ \text{or} \\ p_{i-2,j+2} = 1 \\ \text{or} \\ p_{i-1,j+2} = 1 \end{array} \right\} \text{then, } p_{i-1,j+1} = 1$$

$$\left. \begin{array}{l} p_{i+1,j-2} = 1 \\ \text{or} \\ p_{i+2,j-2} = 1 \\ \text{or} \\ p_{i+2,j-1} = 1 \end{array} \right\} \text{then, } p_{i+1,j-1} = 1 \quad \left. \begin{array}{l} p_{i+1,j+2} = 1 \\ \text{or} \\ p_{i+2,j+2} = 1 \\ \text{or} \\ p_{i+2,j+1} = 1 \end{array} \right\} \text{then, } p_{i+1,j+1} = 1$$

if  $p_{i-2,j} = 1$  then  $p_{i-1,j} = 1$ , if  $p_{i,j+2} = 1$  then  $p_{i,j+1} = 1$ ,  
if  $p_{i+2,j} = 1$  then  $p_{i+1,j} = 1$ , if  $p_{i,j-2} = 1$  then  $p_{i,j-1} = 1$ .

After the regions have been chained, a threshold is applied on the region size. All regions whose pixel number is under the median value of all region sizes are put to zero.



Figure 10: Final binary image and original image

#### 4. RESULTS

The process described in the previous paragraph has been applied to road images presented onto figure 1. Resulting images are given onto figure 10 and 11. The cracks are well detected with more or less noise according to the texture. Thus, on laboratory images (a) and (b) the crack is detected but there is some noise due to a strong texture.

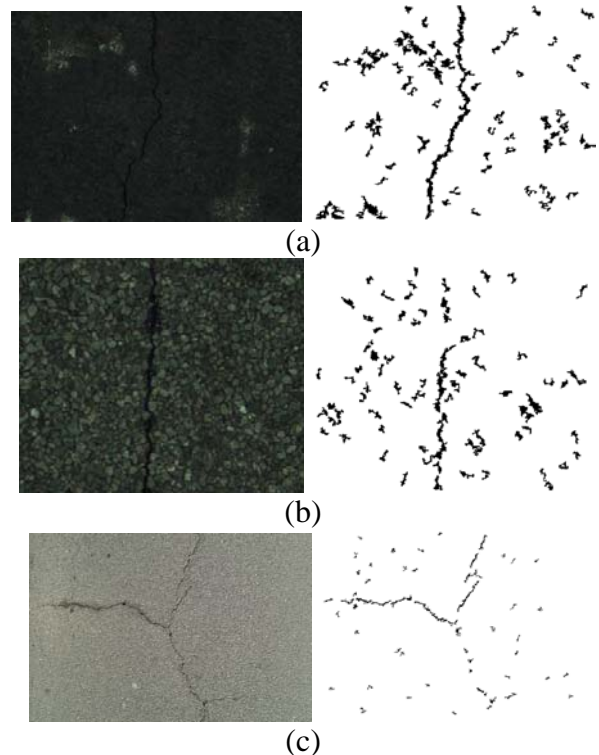


Figure 11: results examples

## 5. CONCLUSIONS AND PERSPECTIVES

In this paper, a wavelet-based image processing method, for pavement crack detection, has been presented. Due to various pavement surface image textures, a matched filtering process was investigated to define the most adapted mother wavelet function. After calculation of a 2D continuous wavelet transform, a complex representation was developed. The angle information allows considering only coefficients that belong to the crack. It is followed by segmentation through scales. A two-step process was developed. First, the maximal values of the wavelet coefficients are searched. Then, their propagation through scales is realized. Finally, a binary image indicating the presence or not of default is obtained.

The processed method to choose the mother wavelet function gives results independent of the pavement texture. Thus, no user intervention is needed. The complex representation allows us to keep only useful information. Finally the two-step segmentation gives a denoised binary image.

In a future work, this method will be evaluated on road images database and rate of false alarm will be computed.

## REFERENCES

- [1] B. Schmidt, *Automated Pavement Cracking Assessment Equipment: State of the Art*, Routes-Roads, World Road Association (PIARC), N°320, October 2003, pp. 35-44.
- [2] C. Rasse, V. Leemans, M.-F. Destains, J.-C. Verbrugge, Application of image analysis to the identification and rating of road surface distress, *Bearing Capacity of Roads, Railways and Airfields*, Correia & Branco 2002, 61 – 68
- [3] Ph. Delagnes, D. Barba, "A markov random field model for rectilinear structure extraction in pavement distress image analysis", 2nd IEEE International Conference on Image Processing (ICIP), Washington DC USA, vol1 pp. 446-449, October 1995.
- [4] P. Subirats, O. Fabre, J. Dumoulin, V. Legeay and D. Barba, "A combined wavelet-based image processing method for emergent crack detection on pavement surface images", 12th European Signal Processing Conference (EUSIPCO), Vienna Austria, pp. 257-260, September 6-10, 2004.
- [5] P. Subirats, J. Dumoulin, V. Legeay and D. Barba, "Enhancement of emergent crack signature on pavement surface images by using a wavelet-based image processing Method", 4<sup>th</sup> workshop on Physics in signal and Image processing, Toulouse, France, 2005
- [6] S. Hermosilla-Lara, P. Y. Joubert, D. Placko, F. Lepoutre, M. Piriou, "Enhancement of open-cracks detection using a principal component analysis/wavelet technique in photothermal non destructive testing", QIRT 2002, Quantitative Infrared Thermography Conference, Dubrovnik (Croatie), 24-27 Septembre 2002, ONERA.
- [7] S. Mallat, *A Wavelet Tour of Signal Processing*, Academic Press, 1998.